

Tunable external cavity quantum cascade laser for the simultaneous determination of glucose and lactate in aqueous phase†

Markus Brandstetter, Andreas Genner, Kresimir Anic and Bernhard Lendl*

Received 16th July 2010, Accepted 11th October 2010

DOI: 10.1039/c0an00532k

A room temperature operated pulsed external-cavity (EC) quantum cascade laser (QCL) was used for mid-infrared (mid-IR) transmission measurements of glucose and lactate in aqueous solution. The high spectral power density of the EC-QCL (ranging from 1–350 mW) over a wide tuning range (1030–1230 cm^{-1}) allowed transmission measurements through optical paths of 130 μm and more. This is a significant improvement in terms of robustness of the measurement setup, especially when samples containing cells or other particles, as is the case for biofluids, are to be analyzed. The broad tuning range furthermore permitted multi-analyte detection based on multivariate calibrations. Promising results on the simultaneous determination of glucose ($c = 0\text{--}800 \text{ mg dL}^{-1}$) and sodium-lactate ($c = 0\text{--}224 \text{ mg dL}^{-1}$) in aqueous solutions in the presence of the interferents maltose and xylose are reported. A partial least squares (PLS) calibration model was calculated which was able to predict the glucose concentration with a root mean square error of prediction (RMSEP) of 9.4 mg dL^{-1} , as proved by external validation. Due to their small size and room temperature operation, EC-QCLs offer an attractive alternative regarding the way mid-IR measurements are carried out. This may be of special importance for new reagent-free bedside monitoring systems.

Introduction

In clinical monitoring of physiologically relevant constituents in bodily fluids, such as glucose and lactate, several different approaches are followed. These can roughly be divided into reagent-based and reagent-free methods. For several reasons, including measurement speed and disposal of medical waste, the reagent-free approach is preferable. A promising approach along this avenue is to apply mid-IR spectroscopy which is able to deliver direct and specific molecular information on the sample under investigation.

Different strategies based on mid-IR spectroscopy have already been investigated in the past.^{1,2} In terms of sampling they can be divided into two categories. Methods in the first category require sampling of the bodily fluids (blood, serum or urine) before measurement. Approaches that fall into the second group aim at non-invasive measurement strategies, where the body is probed from outside through the skin. For the latter methods, mainly photoacoustic spectroscopy in the near-infrared³ or recently also in the mid-IR range⁴ have been proposed, which, while highly interesting, still need to be substantially improved before they may be considered a viable option in medical diagnostics. For the time being it appears that mid-IR based analyzers for reliable clinical diagnostics will focus on aqueous samples.

The major disadvantage associated with performing measurements on aqueous solutions in the mid-IR range is strong water absorption in this spectral region. One counter strategy is to dry the samples prior to the measurement. This dry-film-technology^{1,5} has been widely used but is time-consuming and there are no prospects for *in vivo* applications in the future. A straightforward approach to overcome the strong water absorption is to use short optical pathlengths. In this regard the attenuated total reflection (ATR) technique offers the possibility of small penetration depths (several μm)^{6,7} without putting constraints on the physical design of the ATR based sensor or flow cell.⁸ It should be noted however, that the small optical pathlength also implies a low sensitivity according to Beer's law. Furthermore, it is of utmost importance that the surface of the ATR element is kept clean since the smallest impurities, such as adhered proteins or formed biofilms will contribute to the measured spectra. Thus, when using the ATR technique manual cleaning steps need to be considered after each measurement in order to guarantee constant measurement conditions.⁸

In the case of transmission measurements of aqueous solutions using state of the art Fourier-transform infrared (FTIR) spectrometers furnished with thermal (globar) light sources, the optical path must be kept short. This compromises detection sensitivity and, even more importantly, reduces the robustness of the sensor systems since narrow pathlengths are prone to clogging. An example where this is a particular problem is in the measurement of proteins in the region of the amide I band (around 1640 cm^{-1}). Here the pathlengths may not exceed 8 μm . However, for the quantification of molecules like glucose or lactate, an optical path up to 40–50 μm may be used since these analytes also show characteristic features in the spectral range between 950 and 1250 cm^{-1} where a slightly reduced water absorption is encountered.⁹ Longer optical paths, although

Institute of Chemical Technologies and Analytics, Vienna University of Technology, Getreidemarkt 9/164AC, 1060 Vienna, Austria. E-mail: blendl@tuwien.ac.at; Fax: +43 1 58801 15199; Tel: +43 1 58801 15140

† This article is part of a themed issue on Optical Diagnosis. This issue includes work presented at SPEC 2010 Shedding Light on Disease: Optical Diagnosis for the New Millennium, which was held in Manchester, UK June 26th–July 1st 2010.

desirable from the perspective of a robust measurement configuration, are not practical because there is still significant water background in this spectral region.

A way to improve the robustness and the sensitivity at the same time is to use a more intense light source. The advent of QCLs at the end of the last century made this possibility a viable alternative.¹⁰

QCLs are unipolar lasers based on intersubband transitions between excited states of coupled quantum wells. Because of their cascade structure, QCLs have slope efficiencies that are correlated with the number of stages. Resonant tunnelling acts as a pumping mechanism to achieve population inversion. Unlike other laser sources, the wavelength is determined by quantum confinement, *i.e.* by the thickness of the active layer rather than by the physical properties of the material, giving the flexibility to design lasers emitting in the region of interest and to increase the intensity of the light source.

So far the most frequently used QCLs are distributed feedback (DFB) QCLs where a grating is placed on top of the active semiconductor material to select the desired wavelength of interest. Such lasers can, however, be tuned across a few wavenumbers only. While this is generally sufficient for gas phase measurements, where the analytes have small spectral features, a broader tuning range is required for the analysis of liquids.^{11–13} This is especially true when simultaneous quantitative determinations of several analytes within a complex and changing matrix are performed. An example for such a demanding application would be the concurrent determination of several parameters in bodily fluids such as glucose or lactate, amongst others.

Broadly tunable external-cavity QCLs (EC-QCLs) now offer both high spectral power densities, while covering a large spectral range. In contrast to DFB QCLs, the wavelength selective grating is not placed directly on the QCL chip but is separated by an external cavity in this configuration.¹⁴ Scanning of the grating permits broad tuning ranges of over 200 cm^{-1} . Hence they facilitate multivariate calibrations in multianalyte determinations.^{15–18}

In this paper we introduce a setup for the transmission measurement of aqueous solutions based on a room temperature operated EC-QCL and a thermoelectrically cooled mercury cadmium telluride (MCT) detector, thus avoiding the use of liquid nitrogen with the aim to demonstrate a sensor-like performance of the whole setup. Results on the operation principle and the performance characteristics of the used EC-QCL are shown along with first data on the simultaneous determination of glucose and lactate in aqueous (Ringer) solutions. These molecules are important constituents in bodily fluids since they reflect changes in carbohydrate metabolism.¹⁹ Maltose and xylose were also included since they are common interferences in clinical glucose determination.²⁰ For example, maltose interferences can cause major deviations in test results particularly in the case of patients treated for peritoneal dialysis.

Experimental

Instrumental setup

The experimental setup is shown in Fig. 1. It was designed to be operated at room temperature. The sample solutions containing

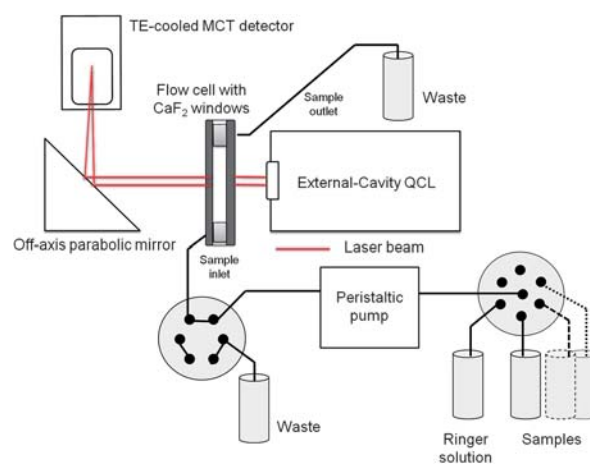


Fig. 1 Schematic representation of the QCL based transmission setup.

the analytes were introduced into the beam path by a standard flow cell (Perkin Elmer, USA) with CaF_2 windows and optical pathlengths of 50, 130 and $200\ \mu\text{m}$ (facilitated by PTFE spacers). Automated sampling was done by a stopped-flow sequential injection analysis (SIA) system consisting of a peristaltic pump (Gilson Inc., USA), PTFE tubings (0.5 mm inner diameter), a selection valve and an injection valve (VICI Valco Instruments, Switzerland). Background spectra of pure Ringer solution were recorded every third sample and the cell was cleaned by rinsing it with ethanol every ten samples. Reference mid-IR spectra were recorded on a Vertex 80v FTIR spectrometer (Bruker Optics, Germany) using a liquid nitrogen cooled MCT detector ($D^* = 4 \times 10^{10}\text{ cm Hz}^{0.5}\text{ W}^{-1}$ at $9.2\ \mu\text{m}$) and a CaF_2 flow cell with an optical path of $50\ \mu\text{m}$.

Tunable mid-IR laser source. The aqueous samples in the flow cell were irradiated by a commercially available pulsed EC-QCL (Daylight Solutions Inc., USA). It offered a maximum peak pulse power of 350 mW at a beam spot size of approximately 2.5 mm on the flow cell. For the acquisition of the absorption spectra the laser was operated in scan-mode, *i.e.* the emission wavenumber was continuously tuned over 200 cm^{-1} between 1030 and 1230 cm^{-1} .

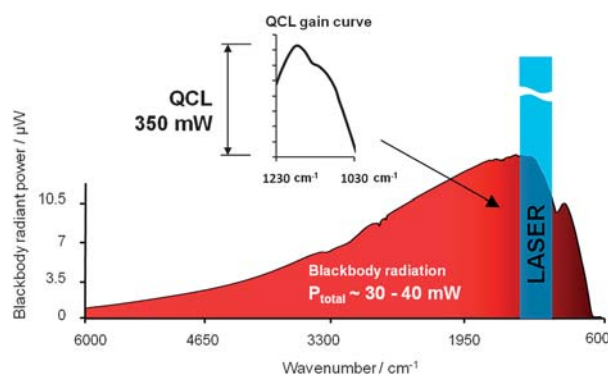


Fig. 2 Schematic comparison of the spectral power densities of a standard FTIR spectrometer furnished with a thermal light source and the situation encountered with the external-cavity QCL used in this work.

A spectral resolution of approximately 1 cm^{-1} was achieved with the EC-QCLs' internal broadband grating. The laser pulse duration was adjusted to 400 ns at a duty cycle of 0.6%.

Fig. 2 shows the prevailing limitations in mid-IR spectroscopy regarding the available optical power. The obtainable power in a FTIR spectrometer is mainly given by the blackbody emission spectrum of the globar. In the sample compartment of a FTIR spectrometer one can measure a remaining radiant power of approximately 30–40 mW for the whole infrared spectral range. In comparison, the employed tunable QCL offered a maximum optical power of 350 mW according to the laser gain curve. However, this power is available within one wavenumber which results in a significantly higher power density than is the case for an FTIR spectrometer.

In the present study during the typical sampling time of 1.2 min, the overall energy transfer to the sample was 0.151 W s (assuming a laser peak power of 350 mW and a 0.6% duty cycle) which is low compared to the situation encountered in a typical FTIR measurement, where the energy transfer amounts to 1.05 W s (assuming 35 mW total blackbody radiation power and 0.5 min sampling time). Structural changes in the samples were therefore not expected and could not be observed during the experiments (see Fig. 3). Using the specific heat capacity of water ($4.18\text{ kJ kg}^{-1}\text{ K}^{-1}$) and assuming no heat dissipation to adjacent regions during a single QCL pulse, the temperature increase of the irradiated sample volume can be calculated to be 52 μK , a value which can be considered negligible.

Room-temperature operated detector. A thermoelectrically cooled MCT detector with a D^* value of $4 \times 10^9\text{ cm Hz}^{0.5}\text{ W}^{-1}$ at $9.2\text{ }\mu\text{m}$ (Infrared Associates Inc., USA) for room-temperature operation was used as the IR detector. The light transmitted through the flow cell was focused on the detector element by a gold plated off-axis parabolic mirror with a focal length of 43 mm.

Data acquisition. All hardware components were controlled by a LabVIEW-based GUI with a server-client programme structure. The detector signal was automatically corrected by an

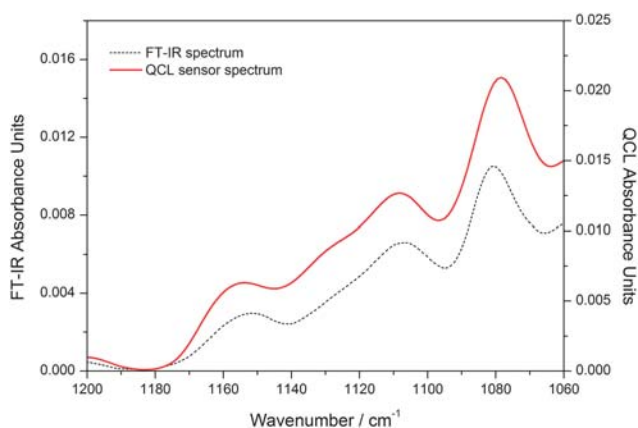


Fig. 3 Glucose solution ($c = 100\text{ mg dL}^{-1}$) measured with the QCL sensor setup (130 μm optical pathlength, solid line) and a conventional FTIR spectrometer (50 μm optical pathlength, dashed line) for comparison.

onboard baseline correction algorithm and the noise was removed by a Fourier-based algorithm. A total of 20 scans was averaged leading to an approximate measurement time of 1.2 min for a single spectrum.

Multivariate data analysis. For multivariate data analysis a PLS regression algorithm was applied to the spectral data using the commercial software PLS Toolbox (Eigenvector Research Inc., USA) for MATLAB (The MathWorks Inc., USA). Data pre-processing of the measured raw data comprised mean centering and 1st derivative. From a total sample set of 170 samples, 120 samples were used for internal and 50 samples for external validation respectively. Internal validation was maintained by cross-validation using random subsets.

Chemicals and sample preparation

Sample solutions were made from stock solutions using D(+)-glucose for biochemistry (Sigma-Aldrich, Germany), sodium-L-lactate puriss. (Sigma-Aldrich), D(+)-maltose monohydrate for biotechnology (Sigma-Aldrich) and D(+)-xylose for biochemistry (Merck, Germany). All samples were prepared in Ringer solution (for injection purposes, Fresenius Kabi, Austria).

Appropriate amounts of stock solution were pipetted into 20 mL glass vials so that the desired final concentration was attained for each analyte. The sample volume required for a single measurement was 0.5 mL. A sample set comprising 170 samples of quaternary solutions was prepared in concentration levels shown in Table 1. The concentration combinations were chosen randomly as evidenced by the corresponding Pearson correlation coefficients summarised in Table 1.

Results and discussion

Characterization of the sensor performance

Prior to the application of the setup for glucose and lactate measurements, several experiments to characterise the setup's operating range were performed. An important parameter in this respect is the noise performance of the optical system. Therefore we measured the overall pulse-to-pulse noise with a particularly large water layer of 200 μm in the beam path.

Table 1 Concentration ranges for the analytes in the quaternary solutions and Pearson correlation coefficients

Analyte	Concentration range (mg dL ⁻¹)
Glucose	0, 20, 50, 100, 200, 400, 800
Na-lactate	0, 11.2, 56, 224
Maltose	0, 8, 16, 24
Xylose	0, 25, 50, 75
Analyte combination	Pearson correlation coefficient
Glucose and Na-lactate	0.08
Glucose and maltose	0.10
Glucose and xylose	0.12
Na-lactate and maltose	0.04
Na-lactate and xylose	0.16

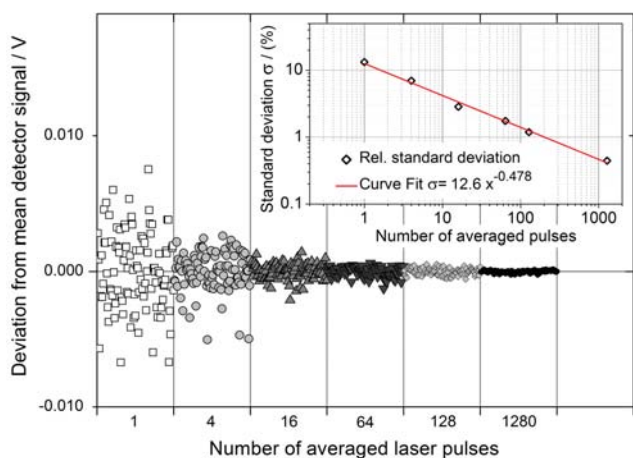


Fig. 4 Characterization of the pulse-to-pulse noise of the detection system at a large optical pathlength (200 μm water layer). The inset shows the decay of the relative standard deviation of the detector signal with increasing number of averages. Data were acquired at an emission wavenumber of 1180 cm^{-1} .

This exceeds the pathlength limits in typical FTIR experiments. Fig. 4 shows the results for different degrees of pulse averaging from 1 (no averaging) to 1280 pulses. For each setting a total of 100 readouts were accumulated. The inset in Fig. 4 illustrates the decay of the relative standard deviation of the measurement with increasing number of averages. The maximum number of averaging was limited to 1280 pulses which was a trade-off between measurement time and the desired accuracy. However, the setting with 1280 averages resulted in a relative standard deviation of 0.4%. In terms of absorbance units (AU) this corresponds to 0.0017 AU.

Although we could show the ability of the setup to deal with aqueous layers of 200 μm thickness at acceptable noise levels, the standard optical pathlength for all subsequent measurements was chosen to be 130 μm . In this configuration the robustness of the setup was still maintained, however, the noise level was

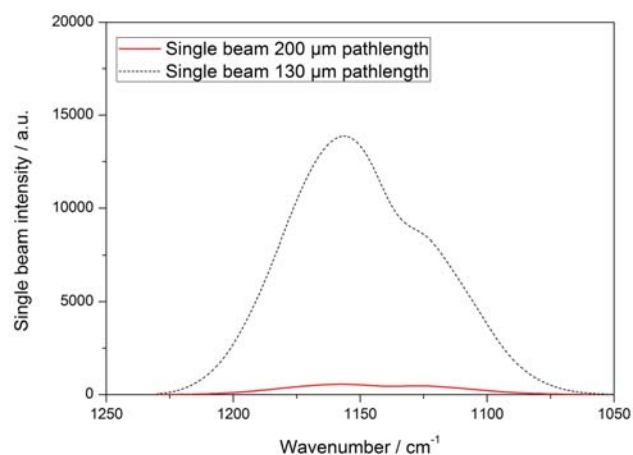


Fig. 5 Single beam intensities for the whole tuning range of the QCL (1030–1230 cm^{-1}) recorded through a water-filled CaF_2 flow cell with an optical path of 130 μm and 200 μm .

significantly reduced to values below 0.0005 AU for the same measurement time.

The results shown in Fig. 5 illustrate the reason for this improvement. One can see there that the single beam intensities were up to 25 times higher for a 130 μm water layer (dashed line) than was the case for 200 μm (solid line).

Comparison of mid-IR spectra recorded with the EC-QCL setup and with a FTIR spectrometer

In order to confirm the ability of the QCL based sensor setup to provide correct absorption spectra, several reference spectra were acquired using an FTIR spectrometer. A comparison of the results for a selected concentration of 100 mg dL^{-1} glucose in Ringer solution is shown in Fig. 3.

The shape and position of the absorption bands recorded using the EC-QCL setup are comparable to the conventional method. It is self-evident that the absolute absorption values must differ due to different optical pathlengths in the setups and the differing offsets in the detection systems employed.

Monivariate analysis of EC-QCL sensor spectra

Having confirmed that the absorption spectra measured with the QCL setup were consistent, we proceeded with the data collection for quantitative analysis. To verify the validity of Beer's law for the QCL sensor setup and to estimate achievable limits of detection, aqueous glucose standards from 0 to 800 mg dL^{-1} were prepared and measured. A linear calibration curve was established by measuring the absorbance at the 1082 cm^{-1} band. Linearity over the whole range was confirmed ($R^2 = 0.9999$, standard deviation of the method $s_{x0} = 2.16 \text{ mg dL}^{-1}$). The corresponding limit of detection (LOD) was calculated as three times the standard deviation of the intercept divided by the slope of the calibration curve and resulted in 3.62 mg dL^{-1} .

Multivariate determination of glucose and lactate by PLS regression analysis

For the establishment of a multivariate calibration model, a set of well defined standards containing the analytes of interest is required. In this study 170 samples were prepared and used for model development and validation. Fig. 6(a) shows the pure analyte spectra comprising the four constituents (Table 1) of the quaternary solutions. Fig. 6(b) shows three selected samples out of the whole calibration set with their individual concentration according to Table 2.

In clinical applications the glucose range for normal persons is between 60 and 110 mg dL^{-1} (on an empty stomach). Values below 40 mg dL^{-1} are called hypoglycemic and values above 180 mg dL^{-1} are called hyperglycemic. In some cases blood-glucose levels can even reach up to 360 mg dL^{-1} for a short time before symptoms become noticeable. However, the operating range of glucose sensors must exceed those values in order to be able to interpret the results correctly. Therefore the sample concentration range was chosen between 0 and 800 mg dL^{-1} for glucose. In the case of lactate the normal values in blood range between 0.55 and 2.2 mmol L^{-1} . Here the measured concentration range was extended to even higher lactate levels to create a stronger interference in the glucose determination.

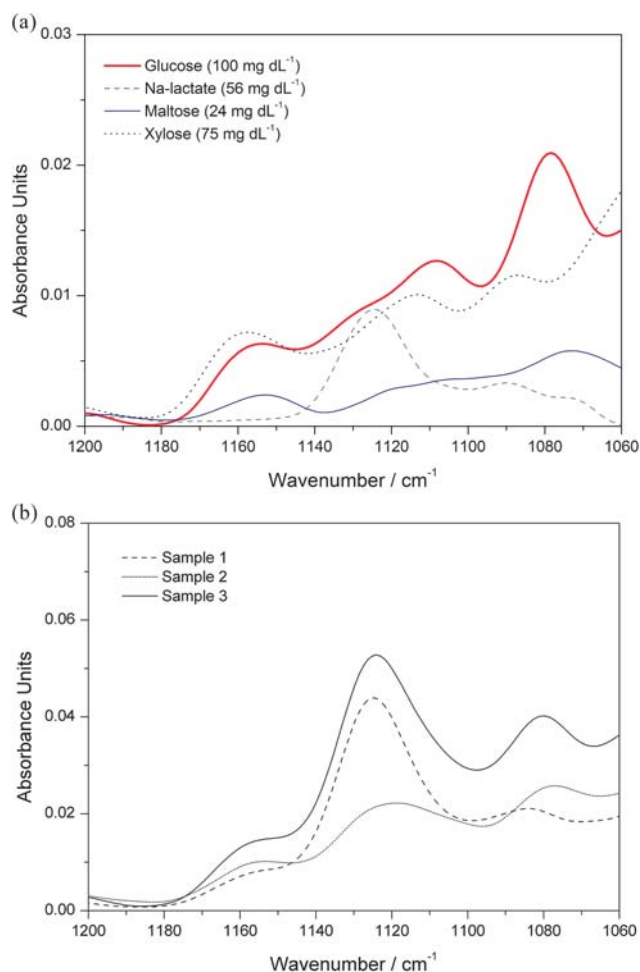


Fig. 6 Absorption spectra of pure analytes dissolved in Ringer solution (a) and quaternary solutions for three selected concentration combinations according to Table 2 (b).

The quality of the resulting calibration models for glucose and sodium-lactate was proved by internal (120 samples) and external (50 samples) validation. The resulting root mean square errors of cross-validation (RMSECV) and prediction (RMSEP) are summarised in Table 3 for two different concentration ranges of glucose (0–400 mg dL⁻¹ and 0–800 mg dL⁻¹).

Optimum calibration and validation results were obtained with five and six PLS factors, respectively. The number of PLS factors chosen for establishing the calibration model was based on the resulting prediction error. In principle, the optimum number of PLS factors is given by the lowest RMSEP as a function of PLS factor. However, in order to avoid overfitting of the data this optimum number was reduced by one.

Table 2 Analyte concentration for sample spectra plotted in Fig. 6

Analyte	Sample 1 (mg dL ⁻¹)	Sample 2 (mg dL ⁻¹)	Sample 3 (mg dL ⁻¹)
Glucose	20	50	100
Na-lactate	224	56	224
Maltose	8	24	24
Xylose	50	25	50

Table 3 Results for the internal and external validation^a

Analyte	Int. validation (RMSECV) (mg dL ⁻¹)	Ext. validation (RMSEP) (mg dL ⁻¹)	PLS factors	Concentration range (mg dL ⁻¹)
Glucose	7.3	9.3	6	0–400
	9.1	9.4	5	0–800
Na-lactate	5.7	6	5	0–224

^a Spectral range: 1060–1230 cm⁻¹; data pre-processing for all spectra: mean centering, 1st derivative; 120 samples internal (cross-validation with random subsets) and 50 samples external validation.

The resulting root mean square errors, RMSECV and RMSEP, were only slightly affected by the different concentration ranges. The required prediction error of <10 mg dL⁻¹ for clinical glucose monitoring was achieved for all ranges.

Since the use of an EC-QCL is still a rather costly undertaking, approaches using a reduced number of selected wavenumbers might be of interest. Based on FTIR data, Heise *et al.* already showed that by variable selection a robust calibration model for glucose in serum can be realised using 4–8 wavenumbers only.²¹ Using QCLs and reducing the number of considered wavenumbers to two, Martin *et al.*²² suggested that the glucose concentration can be determined in serum as well. However, for simultaneous multi-analyte detection in the presence of interferences of varying concentrations, such as maltose and xylose, a widely tunable laser source offers many more possibilities. Furthermore, the achievable RMSEP is improved using a wider wavenumber range (see Table 3).

Another representation of the obtained results for glucose is given by the Clarke error grid analysis (Clarke EGA)²³ in Fig. 7. It is used to quantify the accuracy of glucose meters and is a “gold standard” in clinical analysis. In the Clarke EGA the prediction results obtained by the external validation are plotted against the actual glucose concentration in the sample solutions. The EGA is defined for the typical glucose concentrations in clinical application comprising glucose levels between 0 mg dL⁻¹ and 400 mg dL⁻¹. As is the case for our calibration model all data points are located within region A, *i.e.* they are all within a range of 20% of the reference values. In a clinical setting this would

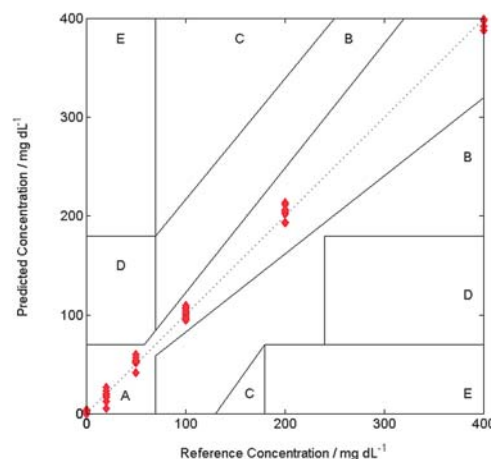


Fig. 7 Clarke EGA for the evaluation of the prediction accuracy of the glucose concentration.

reduce the risk of false positive readings that would lead to incorrect treatment.

Conclusions

A broadly tunable EC-QCL was applied for direct and simultaneous multi-component detection in aqueous solutions. The determination of glucose and lactate in quaternary solutions containing maltose and xylose was reported and showed promising results. The obtained values for RMSECV and RMSEP are in the same range as those obtained by previous studies using bulky FTIR spectrometers furnished with flow-cells of only a few tens of micrometres pathlength,^{9,21} or with ATR elements when analysing blood serum.⁸ However, the high optical power provided by the QCL allowed the use of significantly longer optical paths (130 μm), which is considered a major advantage in terms of long term stability and thus highly promising for potential routine use. Furthermore, the whole setup was small and operated at room temperature.

Future research will focus on the investigation of the effects of additional and higher concentrations of interferents in both aqueous solutions as well as blood serum.

Acknowledgements

The authors gratefully acknowledge the funding within the RSA (Research Studios Austria) programme of the FFG (Austrian Research Promotion Agency).

References

- 1 W. Petrich, *Appl. Spectrosc. Rev.*, 2001, **36**, 181–237.
- 2 H. M. Heise, in *Handbook of Vibrational Spectroscopy*, 2002, pp. 3280–3295.

- 3 G. Spanner and R. Niessner, *Anal. Bioanal. Chem.*, 1996, **355**, 327–328.
- 4 H. von Lilienfeld-Toal, M. Weidenmüller, A. Xhelaj and W. Mänteles, *Vib. Spectrosc.*, 2005, **38**, 209–215.
- 5 G. Deleris, *Vib. Spectrosc.*, 2003, **32**, 129–136.
- 6 H. M. Heise, R. Marbach, G. Janatsch and J. D. Kruse-Jarres, *Anal. Chem.*, 1989, **61**, 2009–2015.
- 7 N. J. Harrick and F. K. du Pré, *Appl. Opt.*, 1966, **5**, 1739.
- 8 G. Hoşafçı, O. Klein, G. Oremek and W. Mänteles, *Anal. Bioanal. Chem.*, 2007, **387**, 1815–1822.
- 9 R. Vonach, J. Buschmann, R. Falkowski, R. Schindler, B. Lendl and R. Kellner, *Appl. Spectrosc.*, 1998, **52**, 820–822.
- 10 J. Faist, F. Capasso, D. L. Sivco, C. Sirtori, A. L. Hutchinson and A. Y. Cho, *Science (New York, N. Y.)*, 1994, **264**, 553–556.
- 11 A. A. Kosterev and F. K. Tittel, *Quantum Electron.-Special Issue QC Lasers*, 2002, **38**, 582–591.
- 12 R. F. Curl, F. Capasso, C. Gmachl, A. A. Kosterev, B. McManus, R. Lewicki, M. Pusharsky, G. Wysocki and F. K. Tittel, *Chem. Phys. Lett.*, 2010, **487**, 1–18.
- 13 S. Schaden, A. Domínguez-Vidal and B. Lendl, *Appl. Phys. B: Lasers Opt.*, 2007, **86**, 347–351.
- 14 G. Wysocki, R. Lewicki, R. F. Curl, F. K. Tittel, L. Diehl, F. Capasso, M. Troccoli, G. Hofler, D. Bour, S. Corzine, R. Maulini, M. Giovannini and J. Faist, *Appl. Phys. B: Lasers Opt.*, 2008, **92**, 305–311.
- 15 A. Hugi, R. Maulini and J. Faist, *Semicond. Sci. Technol.*, 2010, **25**, 083001.
- 16 A. Hugi, R. Terazzi, Y. Bonetti, A. Wittmann, M. Fischer, M. Beck, J. Faist and E. Gini, *Appl. Phys. Lett.*, 2009, **95**, 061103.
- 17 A. Mohan, A. Wittmann, A. Hugi, S. Blaser, M. Giovannini and J. Faist, *Opt. Lett.*, 2007, **32**, 2792.
- 18 R. Maulini, A. Mohan, M. Giovannini, J. Faist and E. Gini, *Appl. Phys. Lett.*, 2006, **88**, 201113.
- 19 K. B. Storey, *Functional Metabolism: Regulation and Adaptation*, Wiley-IEEE, 2004.
- 20 T. G. Schleis, *Pharmacotherapy*, 2007, **27**, 1313–1321.
- 21 H. M. Heise, U. Damm, O. Vogt and V. Konderpati, *Vib. Spectrosc.*, 2006, **42**, 124–129.
- 22 W. B. Martin, S. Mirov and R. Venugopalan, *J. Biomed. Opt.*, 2002, **7**, 613–617.
- 23 W. L. Clarke, D. Cox, L. A. Gonder-Frederick, W. Carter and S. L. Pohl, *Diabetes Care*, 1987, **10**, 622–628.